

Integration of Large-Scale Simulations and Numerical Modelling Tools in Close Link with the LHD Experiment^{*)}

Masayuki YOKOYAMA, Ryosuke SEKI, Chihiro SUZUKI, Masahiko EMOTO, Katsumi IDA,
 Masaki OSAKABE, Sadayoshi MURAKAMI¹⁾, Yasuhiro SUZUKI, Shinsuke SATAKE,
 Masanori NUNAMI, Atsushi FUKUYAMA¹⁾, Hiroshi YAMADA,
 Numerical Simulation Research Project and LHD Experiment Group

National Institute for Fusion Science, Toki 509-5292, Japan

¹⁾*Department of Nuclear Engineering, Graduate School of Engineering, Kyoto University, Kyoto 615-8540, Japan*

(Received 10 December 2013 / Accepted 20 January 2014)

An integrated transport analysis suite, TASK3D-a, has been developed with the emphasis on establishing close-link with the LHD experiment database. The suite makes possible energy transport analyses for huge cases, from which the systematic understandings can be elucidated. A statistical approach for implementing large-scale simulation results into the integrated modelling has been tested. The importance of strengthening trilateral links among experiments, large-scale simulations, and integrated numerical modelling tools such as TASK3D, is crucial for promoting systematic understandings, performing validations, and then increasing the predictive capabilities.

© 2014 The Japan Society of Plasma Science and Nuclear Fusion Research

Keywords: TASK3D-a, LHD, energy confinement, Kaiseki Data Server, large-scale simulation

DOI: 10.1585/pfr.9.3402017

1. Introduction

The Large Helical Device (LHD) has steadily extended its parameter regime [1]. More importantly, not only the parameter extension, but also the increased diagnostic capability has provided a wide-range database to be exploited for the accurate physics discussion. Simultaneously, cutting-edge large-scale simulations of LHD plasmas have been conducted for their validation by direct comparisons with experimental observations [2, 3].

However, cases for such comparisons have been limited to a relatively small number because of the large size of cutting-edge simulations. To acquire comprehensive physics understandings and then increase the predictive capabilities, systematic and comprehensive comparisons should be performed between experiments and theory/simulations. Therefore, simplified numerical modelling tools developments are complimentary essential so that the experiment database can be widely and effectively exploited.

One such tool is the integrated transport analysis suite, TASK3D-a (analysis version) [4], which has been developed as a first attempt for conducting automated energy confinement analyses for NBI plasmas in LHD. The capability of TASK3D-a has been gradually increasing from its first version TASK3D-a01 (released in Sep. 2012) through implementations of modules for neoclassi-

cal transport (GSRAKE [5]), ECH deposition, and neutral penetration from the plasma periphery, etc., although describing these extensions is not the main topic of this paper. In this paper, the significance and usefulness of TASK3D-a are described in terms of its close link with LHD experiment data, thereby making systematic analyses possible. An on-going trial is introduced for integrating cutting-edge large-scale gyrokinetic simulation results into TASK3D before presenting a summary and outlook in Section 5. Such integrations should significantly enhance systematic validations of large-scale simulation results against the wide-range experiment database.

2. TASK3D-a in the LHD Experiment

The computational flow in TASK3D-a01 has been already introduced in Ref. [4, 6] and it is not repeated here. In brief, the equilibrium specification, NBI deposition, and energy balance calculations are packaged so that they are sequentially executed in an automated manner. The package contains an LHD experiment data interface that has a direct link to the so-called LHD Kaiseki (analysis in Japanese) Data Server [7] and TSMAP (real-time coordinate mapping system) [8]. Processed diagnostics data are registered onto the Kaiseki Data Server in a common format (ASCII file, the so-called *eg*-format), and then profile data, such as temperature and density profiles (which are required for transport analyses), are mapped from the real geometry to the effective minor radius, r_{eff} , defined by TSMAP. These mapped profile data are then transferred as

author's e-mail: yokoyama@LHD.nifs.ac.jp

^{*)} This article is based on the invited presentation at the 23rd International Toki Conference (ITC23).

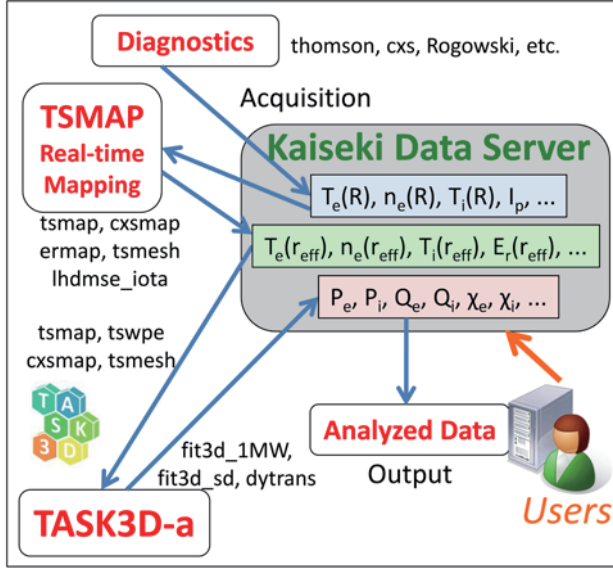


Fig. 1 Schematic illustrating the close link between TASK3D-a and LHD experiment data (centralized to LHD Kaiseki Data Server).

input to TASK3D-a. Some TASK3D-a results (NBI deposition profiles, ion and electron heat diffusivities, etc.) are then registered onto the Kaiseki Data Server for common use. To utilize these results, users just need to login to the Kaiseki Data Server. The dataflow described above is conceptually illustrated in Fig. 1. The words written in small characters are the names of registered data (so-called *eg* data).

3. Transport Analyses Database Created by TASK3D-a

The process described in Section 2 shows how TASK3D-a has been fully integrated into the LHD experiment database, allowing smooth utilization of LHD experiment data and then increasing numbers of analyses. So far, extensive analyses have been performed on high ion temperature (T_i) plasmas [9] ($T_i \sim 5 - 7$ keV, $T_i > T_e$ at the core with the density of $1 \sim 2 \times 10^{19} \text{ m}^{-3}$), and on medium-to-high density plasmas [10] ($T_i \leq T_e \sim 3 - 4$ keV at the core with the density of $3 \sim 5 \times 10^{19} \text{ m}^{-3}$) have been extensively analyzed. High- T_e plasmas will also be analyzed once ECH modules are fully integrated into TASK3D-a. For super high-density core plasmas [11] and high-beta [12] plasmas, MHD equilibrium should be more carefully treated by HINT2 [13], including such as stochasticization; these are tasks beyond the presently implemented VMEC [14] in which the existence of nested magnetic surfaces is assumed *a priori*. Note that high- T_i and medium-to-high density plasmas have volume-averaged beta values typically of at the most 1%, where VMEC equilibria should be considered to be reasonable. Fast computation of VMEC is also an advantage for integrated analyses.

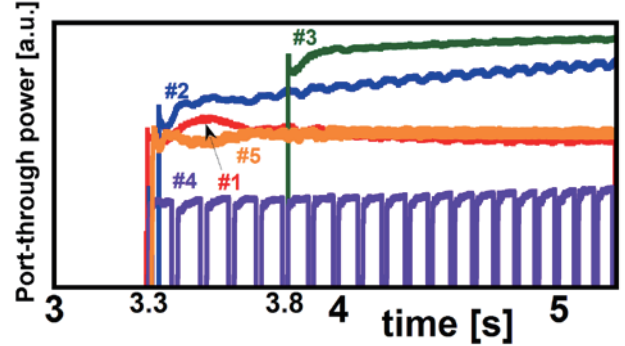


Fig. 2 Example of NBI injection pattern.

Figure 2 shows an example NBI injection pattern (port-through power) of an LHD shot. In this shot, all five NBIs were injected (#1, #2, #4 and #5 from 3.3 s, and then #3 from 3.8 s). One beam line (#4) was intentionally modulated on purpose for the charge exchange spectroscopic (CX) measurement (for subtracting background signal), from which the T_i profile can be obtained. In this shot, T_i profiles can be measured at 100 ms intervals. Thus, for this particular shot, 20 timings can be analyzed with full sets of temperature and density profiles. In this manner, the numbers of TASK3D-a analyses have been increased. So far, on the order of 10^4 cases have been analyzed from multiple shots, including cases without T_i profile measurements (only T_e and n_e are available). The important feature of such a huge TASK3D-a analysis database is that it stores plasma parameters, experimental power balance, neoclassical diffusion, and dimensionless parameters, *etc.*, “ALL IN PROFILES.” Thus, it is anticipated that one is able to deduce heat diffusivity scaling with radial dependence, with distinguishing ion and electron channels using a statistical approach. This is one of research targets for the near future and will be reported in a separate paper. It should go far beyond the global energy confinement scaling [15, 16], and thus the significant increase in the predictive capabilities is expected. Such a deduced scaling will be implemented into TASK3D-p, the predictive version of TASK3D in which transport models (e.g., χ_i and χ_e) become “the inputs” rather than the outputs as in the case of TASK3D-a.

In the following text, some examples of systematic plots on energy transport analyses are introduced as the significance of the TASK3D-a analyses database. For simplicity, the plotted data are only a small part (~ 1%) of the entire database.

Based on dynamic transport analyses, Fig. 3 (a) shows the ion and electron heat diffusivities as a functions of the temperature ratio, T_e/T_i , for $r_{eff}/a_{99} \sim 0.4$. Here a_{99} is the plasma minor radius in which 99% of the total stored energy is confined. In general, data for $T_e/T_i < 1$ correspond to high- T_i plasmas (larger symbols), and those for $T_e/T_i > 1$ correspond to medium-to-high density plasmas

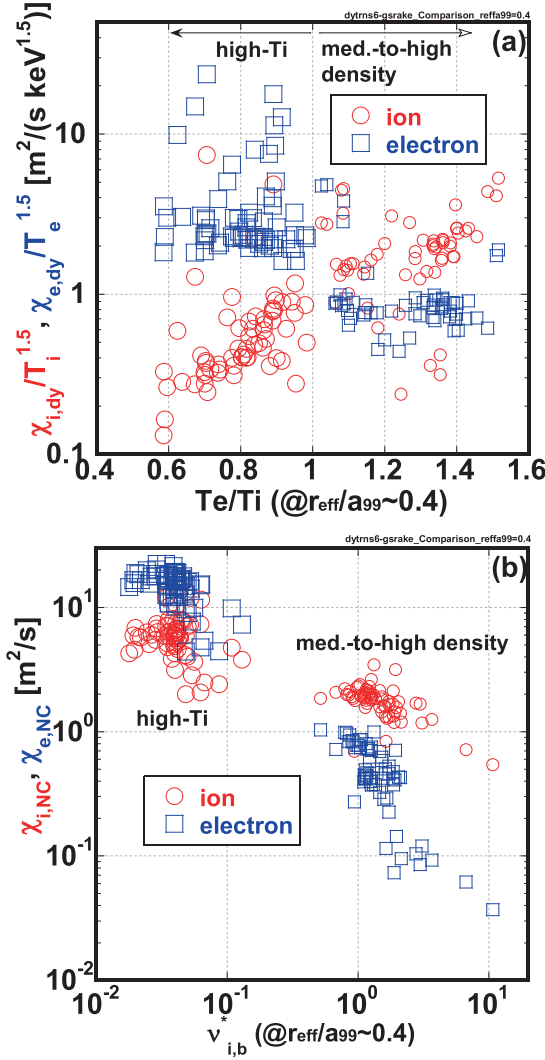


Fig. 3 Example figures describing systematic dependence based on TASK3D-a analysis database (multiple shot-timings). (a) Ion and electron heat diffusivity evaluated with the dynamic transport as a function of temperature ratio, T_e/T_i at a specific radius ($r_{eff}/a_{99} \sim 0.4$). (b) Ion and electron neoclassical heat diffusivities as a function of normalized ion collision frequency. The larger symbols correspond to high- T_i plasmas, and smaller to medium-to-high density plasmas.

(smaller symbols). The diffusivity is normalized by Gyro-Bohm temperature scaling, $T^{1.5}$. The tendency is recognized that the normalized ion (electron) heat diffusivity decreases (increases) as T_e/T_i is decreased. Thus, it can be considered that present high- T_i plasmas in LHD are situated in a T_e/T_i regime with smaller ion diffusivity but with larger electron diffusivity. This systematic plot implies that plasmas with $T_e \sim T_i$ are favorable in terms of simultaneously small ion and electron heat diffusivity. This implication is consistent with recent trials for increasing T_e in high- T_i plasmas (from $T_i > T_e$ towards $T_i \sim T_e$) through the increase of available ECH power.

In addition to the experimental energy balance, TASK3D-a also evaluates neoclassical heat diffusivity (in-

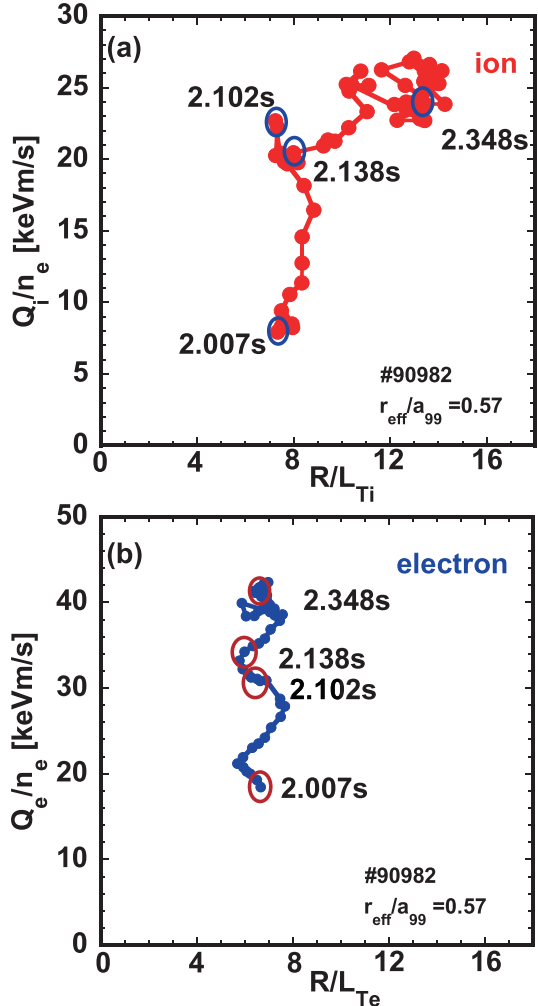


Fig. 4 (a) Ion and (b) electron heat flux divided by the electron density as a function of the normalized scale length of inverse of each temperature gradient at $r_{eff}/a_{99} = 0.57$ (inside the ion ITB of high- T_i plasma) [reproduced from Fig. 3 in Ref. [17]].

cluding the effects of neoclassical ambipolar radial electric field) in addition to experimental power balance. Figure 3 (b) shows the ion and electron neoclassical heat diffusivities as a function of ion collisionality, which is normalized by the ion collision frequency at the banana-plateau boundary. This plot shows clear separation between high- T_i plasmas (lower $v_{i,b}^*$) and medium-to-high density plasmas (higher $v_{i,b}^*$) in terms of the normalized collision frequency. For electrons, the variation of heat diffusivity with collisionality is larger than that for ions. These plots are merely examples of systematic plots that can be extracted from the TASK3D-a analyses database. As mentioned above, statistical analysis would be one of approaches for exploiting the database to elucidate systematic and comprehensive understandings of energy transport properties in LHD.

Figure 4 shows another example that clearly displays the powerfulness of TASK3D-a. The figure shows the tem-

poral behavior of (a) ion and (b) electron heat diffusivities (divided by the electron density) as a function of normalized scale length of the ion and electron temperature gradient [17]. These plots are for a radius inside the ion internal transport barrier of LHD high- T_i plasma (#90982) in the phase (duration of about 300 ms) of increasing T_i . The plots consist of data for 58 timings, all of which were evaluated with TASK3D-a; profile fittings, equilibrium specifications, NBI deposition calculations (including slowing down effect), dynamic transport analyses taking into account the T_i profile measured by CXS with a higher time resolution (~ 20 ms), and temporally interpolated values from those. Figure 4(a) clearly identifies the time of ion energy confinement improvement, which occurs at about 2.14 s. Before this time, R/L_{Ti} is almost unchanged even with a large increase in Q_i/n_e . In contrast, after 2.14 s, R/L_{Ti} becomes nearly doubles (the temperature gradient becomes about twice as steep) with almost no change in Q_i/n_e . However, there is no such confinement improvement observed in the electron channel (see Fig. 4(b)). In such a way, TASK3D-a can also provide sequential information on energy confinement properties through dynamic transport, which also extends the analyses database.

4. Approach for Implementing Large-Scale Simulation Results into TASK3D-p

Sections 2 and 3 describe how TASK3D-a has been useful for experimental analyses. On the other hand, the predictive version, TASK3D-p, has been developed to predict, e.g., the achievable temperature (and those profiles) based on assumed heating scenario and transport model.

Recently, ITG-turbulence-induced ion heat diffusivity in an LHD high- T_i plasma has been estimated [18] through the gyrokinetic simulation code, GKV-X, in which experimentally observed profiles and corresponding three-dimensional VMEC equilibrium are employed. In such a way, direct application of a cutting-edge large-scale simulation to experiment has been progressed. However, in terms of wide-range experiment database in LHD as mentioned above, this application can be recognized as merely “one timing of one shot”.

Because it is extremely time-consuming to run nonlinear gyrokinetic simulations over a wide-range of plasma parameters, a novel reduced-model has been deduced in Ref. [19], in which nonlinear gyrokinetic simulation results can be predicted from “less-expensive” linear simulations. The deduced model for ITG-turbulence-induced ion heat diffusivity is represented through the linear ITG growth rates and zonal flow decay times, both of which are available from linear gyrokinetic simulations. In this way, the implementation of ITG-turbulence-induced ion heat diffusivity into numerical modelling, such as TASK3D-a, can be considered as pointed out in Ref. [19].

However, even in this reduced model, it still requires

linear gyrokinetic simulations. In terms of TASK3D-p development, an on-going trial for further reduction is described below. In Ref. [19], 21 nonlinear gyrokinetic simulation results were treated taking the following as parameters: radial position, safety factor, magnetic shear, normalized scale lengths of ion-temperature, and density gradient (cf., Table 1 in Ref. [19]). A multivariate nonlinear regression analysis was applied to this dataset by taking the latter four parameters as predictor variables. The remaining parameter, radial position, would be replaced by the effective helicity [20], because it is one of the quantities for describing the three-dimensionality of magnetic configurations. Including this parameter will be performed with further implementation of other possibly important parameters, such as dimensionless collisionality, Larmor radius, etc. Thus, the current result shown below should be considered as a first example for reduced modelling through a statistical approach.

A multivariate nonlinear regression analysis performed on the 21 GKV-X data has provided the following functional form for the Gyro-Bohm normalized nonlinear gyrokinetic simulations results:

$$\chi_{i,\text{Fit}}/\chi_{i,\text{GB}} = 0.03856 \left(\frac{R_0}{L_{Ti}} \right)^{1.758} \left| \frac{R_0}{L_n} \right|^{0.0506} \times |\beta|^{-0.285} \left(\frac{\iota}{2\pi} \right)^{-1.567}, \quad (1)$$

where $\iota/2\pi$ is the rotational transform (the inverse of the safety factor). Figure 5 compares the ion heat diffusivity from the GKV-X nonlinear simulations (vertical axis) and the fitted values obtained from eq. (1). The GKV-X results are reasonably well reproduced, although some scatter appears, especially in small values of the ion heat diffusivity (cf., to be compared to Fig. 9 in Ref. [19]). Nonetheless, the important point about eq. (1) is that all the predictor variables can be estimated from only equilibrium and density/temperature profiles. Note that this is based on a purely statistical approach, and a physical interpretation of eq. (1) is yet to be pursued. Nevertheless, a relation such as eq. (1) makes it much easier to implement a model for ITG-turbulence-driven ion heat diffusivity into TASK3D-p through such a fitting formula.

5. Summary and Outlook

A wide-range experiment database has been accumulated in LHD, as has been done at other fusion experiment devices. Cutting-edge large-scale simulations in various areas of physics topics have been performed to validate the simulations themselves and increase physics understandings. However, links between experiment and large-scale simulation have been relatively limited, partly due to the large size of the computations. To strengthen this weak link, it is crucial to develop simpler numerical modelling tools. In this paper, the integrated transport analysis suite, TASK3D, has been described as a promising development

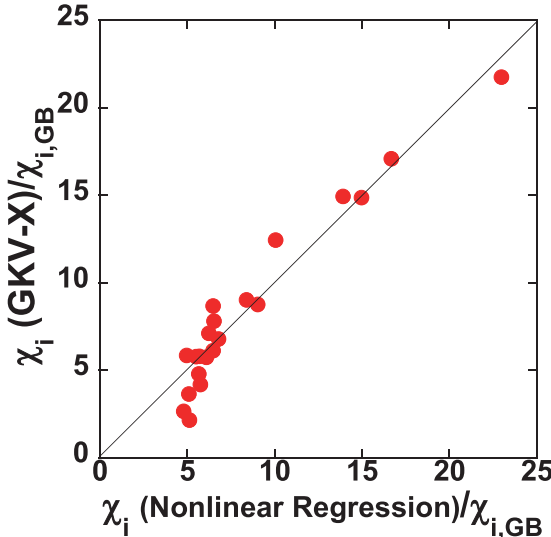


Fig. 5 Comparison of the ion heat diffusivities from GKV-X nonlinear simulations (vertical axis) and the nonlinear regression results (estimated by eq. (1), horizontal axis).

for LHD plasmas. This tool can be extended to other experiments.

The close link between TASK3D-a and the experiment database (LHD Kaiseki Data Server) has enabled extensive energy transport analyses in NBI-heated LHD plasmas possible. So far, on the order of 10^4 analyses cases have been accumulated. General tendencies of energy confinement properties in LHD have been elucidated from only a part of that database. In the near future, this TASK3D-a analyses database will be utilized in statistical analyses to deduce such as ion and electron heat diffusivity scaling with radius dependence; the results will be reported in a separate paper.

Efforts have also been made for implementing large-scale simulation results into numerical modelling tools. A reduced model for the ITG-turbulence-induced ion heat diffusivity has been obtained in Ref. [19] in this regard. In this paper, another trial is introduced; a trial based on the multivariable nonlinear regression analysis, with predictor variables available from the temperature and density profiles and equilibrium. Of course, the eq. (1) obtained from this approach should be further upgraded and improved by adding other predictor variables that possibly affect ITG modes. Nevertheless, these efforts should strengthen links between experiment and large-scale simulation through integrated modeling, such as TASK3D.

On the basis of this enhanced trilateral integration among experiment, large-scale simulations, and integrated numerical modelling tools, systematic physical understandings and validations can be significantly enhanced, and then the predictive capabilities can also be increased.

Acknowledgments

The authors are grateful to LHD experiment group for making the experimental data available. Encouragements and advices from Prof. H. Sugama (National Institute for Fusion Science) have been highly appreciated. This work has been supported by the NIFS Collaborative Research Programs, NIFS11KNTT008 and NIFS11UNTT006. One of authors (M.Y.) appreciates a grant-in-aid from the Future Energy Research Association. Strong support from Dr. Andreas Kus (Max-Planck institute for Plasma Physics, Greifswald, Germany) on the statistical analysis of GKV-X data is highly appreciated.

- [1] O. Kaneko, H. Yamada *et al.*, Nucl. Fusion **53**, 104015 (2013).
- [2] H. Yamada for LHD Experiment Group., O4-1, presented at 22nd International Toki Conference (Nov. 2012).
- [3] For example: NIFS Peer Review Report in FY2012, http://www.nifs.ac.jp/hyokarep/gaibuhyouka_24.pdf (in Japanese).
- [4] M. Yokoyama *et al.*, Plasma Fusion Res. **8**, 2403016 (2013).
- [5] C.D. Beidler and W.D. D'haeseleer, Plasma Phys. Control. Fusion **37**, 463 (1995).
- [6] M. Yokoyama for TASK3D Users and Developers, NIFS-MEMO-61, National Institute for Fusion Science, Nov. 2012.
- [7] M. Emoto *et al.*, Fusion Eng. Des. **81**, 2019 (2006).
- [8] C. Suzuki *et al.*, Plasma Phys. Control. Fusion **55**, 014016 (2013).
- [9] K. Nagaoka *et al.*, Nucl. Fusion **51**, 083022 (2011).
- [10] A. Dinklage, M. Yokoyama *et al.*, Nucl. Fusion **53**, 063022 (2013).
- [11] R. Sakamoto *et al.*, Fusion Sci. Technol. **58**, 53 (2010).
- [12] Y. Suzuki *et al.*, Nucl. Fusion **53**, 073045 (2013).
- [13] Y. Suzuki *et al.*, Nucl. Fusion **46**, L19 (2006).
- [14] S.P. Hirshman and J.C. Whitson, Phys. Fluids **26**, 3553 (1983).
- [15] For example, ITER Physics Basis, Nucl. Fusion **39**, 2175 (1999).
- [16] H. Yamada *et al.*, Nucl. Fusion **45**, 1684 (2005).
- [17] K. Ida *et al.*, Phys. Rev. Lett. **111**, 055001 (2013).
- [18] M. Nunami *et al.*, Phys. Plasmas **19**, 042504 (2012).
- [19] M. Nunami *et al.*, Phys. Plasmas **20**, 092307 (2013).
- [20] M. Yokoyama and K.Y. Watanabe, Nucl. Fusion **45**, 1600 (2005).